

VAPING WITH NICOTINE REDUCES LEFT VENTRICULAR CARDIAC FUNCTION
IN ADOLESCENT MALE MICE

Undergraduate Honors Thesis

Submitted in Partial Fulfillment of the Requirements for Graduation with *Honors*
Research Distinction in Biomedical Science in the College of Medicine, Department of
Biomedical Education and Anatomy at The Ohio State University

Evan Neczypor

Undergraduate Biomedical Science Major

Class of 2021

Undergraduate Honors Thesis Committee Members:

Dr. Loren Wold, PhD

Dr. Kristin Stanford, PhD

Dr Claudia Mosley, PhD

Defense Date: March 29th, 2021

<u>Table of Contents:</u>	Page
Acknowledgements	iii
List of Figures and Tables	iv
Abstract	v
Introduction	1-2
Results and Discussion	3-11
Conclusions	11-12
Materials and Methods	12-18
References	21-24

Acknowledgements:

Dr. Loren Wold and Dr. Matthew W. Gorr served as excellent mentors for this project. I would like to thank Dr. Wold for entrusting me as the leader of this project and providing endless support. My time in the Wold lab has been transformational and has helped shape my career goals and interests. I am thankful to Dr. Wold for always believing in me and pushing me to be my best, and for his commitment to supporting undergraduate students like myself, both professionally and personally. I would also like to thank Dr. Gorr who was invaluable to this project from start to finish. Dr. Gorr was always available to discuss new targets, experiments, timepoints, and data analysis. Dr. Gorr is an incredible teacher who not only helped me learn many of the techniques I needed for this project, but also helped me learn to always seek to understand our methodology and think critically about the direction of our project.

Additionally, my success with this project would have been insignificant if not for the help and support of my fellow lab members, including Matthew Mears, Neill Schwieterman, David Aslaner, Jacob Grimmer, Drew Miller, Michael Muffler and Yael Escobar, all of whom were indispensable for their contributions and their willingness to help me learn techniques and troubleshoot experiments.

Lastly, thank you to all others who played a role in my research experience. Thank you to our collaborators, Dr. Gang Chen and Dr. Philip Lazarus for their work on this project. Thank you to the leaders of the Biomedical Science program, Dr. John Gunn and Steven Mousetes, for helping me navigate my experience at The Ohio State University. Thank you to my committee members, Dr. Stanford and Dr. Mosley for helping me along this process.

<u>List of Figures:</u>	Page
<i>Figure 1: Body Weights</i>	4
<i>Figure 2: Left Ventricular Echocardiography</i>	5
<i>Figure 3: Assessment of Cardiac Fibrosis</i>	7
<i>Figure 4: Assessment of Systemic and Cardiac Biomarkers</i>	9
<i>Figure 5: Nicotine Metabolism</i>	11
<i>Supplemental Figure 1: Additional Measures of Global Cardiac Function</i>	19
<i>Supplemental Figure 2: Cardiomyocyte Function</i>	20

Abstract

Electronic cigarettes (ECs) are the most commonly used tobacco product by teens and young adults. The aim of this study was to determine the potential effects of EC exposure on cardiac health in adolescent mice. Four-week-old FVB mice were exposed to EC vapor with 20.2 mg/mL of nicotine or vehicle alone for either 3 weeks or 3 months. Mice were exposed to HEPA-filtered air as a control (FA). Body weight was significantly reduced in mice exposed to EC vapor with nicotine versus mice exposed to the EC vehicle or to the FA control. Echocardiography revealed that male, adolescent mice displayed reductions in fractional shortening and impaired diastolic function after exposure to EC with nicotine, but not in response to vehicle alone. RT-qPCR demonstrated that EC exposure with nicotine caused an increase in left-ventricular *COL1A1*, and *COL3A1* expression after 3 weeks of exposure, but this was reversed after 3 months of exposure. Trichrome staining showed increased vascular fibrosis following exposure to the EC vehicle for 3 months. Male mice exposed to EC vapor with nicotine had elevated serum concentrations of 3 inflammatory cytokines and 2 growth factors. While serum nicotine concentrations in male and female mice exposed to EC with nicotine were similar, concentrations of multiple metabolites were significantly lower in females. Further, the 3-hydroxycotinine/cotinine metabolite ratio, a measure of enzymatic nicotine metabolism (CYP2A5 activity), was significantly higher in females vs males. Further RT-qPCR targeting liver Cyp2A5 also showed increased expression in females vs males, suggesting a more rapid rate of enzymatic nicotine metabolism in females. These results heighten the concern for the dangers of EC use, specifically in youth, and call for further work detailing the mechanistic contributions to the observed reduction in cardiac function. The novel results of this study demonstrate that EC vapor exposure with nicotine can reduce cardiac function in developing male mice.

Introduction

Electronic cigarettes (ECs) are the most commonly used tobacco product by middle and high school aged children.¹ Alarming, a recent study found that use among this age group continues to increase yearly, with 9% of 8th graders, 20%, of 10th graders, and 25% of 12th graders having used EC products in the past month.² With these rates in mind, there is significant concern as to whether exposure to hazardous inhalants found in EC vapor can cause damage during the sensitive window of development in school-aged children. Overall, the prolific usage of ECs has not been met with sufficient data to demonstrate its toxicity or relative safety to health.

Although the field of EC research is still in its infancy, the developing body of literature invokes significant concern into the pulmonary and cardiovascular health effects of EC use. One clinical study found that EC use by adolescents is associated with increased symptoms of chronic bronchitis.³ Several other clinical and rodent studies have connected EC use to pulmonary inflammation, as evidenced by immune cell infiltration and increased inflammatory cytokines in bronchiolar lavage fluid.^{4,5} Furthermore, clinical studies have found impaired respiratory function and gas exchange in EC users.^{5,6} While the majority of EC research has been dedicated to the lungs, cardiovascular effects in users have also been reported. Notably, alterations in arterial function and integrity, and increased platelet aggregation, leading to thrombotic events, have been observed in rodent and human studies.⁷⁻¹¹ Unlike these vascular findings, the cardiac effects of EC exposure remain largely uncharacterized. Several studies have noted that chronic EC exposure in adult rodents does not alter cardiac function,^{12,13} but investigation for more subtle abnormalities, especially in developing rodents, is severely lacking.

Other sources of inhaled particulates and noxious gasses, such as traditional cigarettes and air pollution, have been established as major contributors to cardiac pathophysiology. Exposure to

these inhalants has been linked to adverse cardiac outcomes characterized by inflammation, oxidative stress, and fibrosis.^{14–16} The production of many similar byproducts from the combustion of EC liquids raises concern into potential parallels between EC exposure and these established environmental triggers of disease. The composition of EC liquid includes nicotine, flavorings, and a vehicle of propylene glycol and vegetable glycerin, both of which have been deemed “generally recognized as safe” by the FDA for oral consumption, but not for combustion and subsequent inhalation.¹⁷ This heat combustion process is responsible for the formation of several presumably toxic byproducts, including reactive organic compounds, and fine particles (PM_{2.5}) which have a diameter less than 2.5 μm .^{18,19} The small size of these particles allows for deep lung penetration, alveolar deposition, and entrance into pulmonary and systemic circulation, resulting in direct interaction with the heart.^{19–21} We have previously demonstrated that exposure to airborne PM_{2.5} during sensitive windows of development causes long term cardiac dysfunction in mice.^{22,23}

In this study, we sought to investigate whether an “adolescent” mouse model of EC exposure shows an altered cardiac phenotype. Here, we show that youth mice (1-month-old) exposed to EC vapor with nicotine for 3 months have significantly reduced left ventricular (LV) systolic and diastolic cardiac function, in males but not females, demonstrating for the first time an effect of vaping on cardiac function in wild type mice. These data were paired with changes in cardiac gene expression related to fibrosis/inflammation and sex-specific alterations in levels of inflammatory cytokines, growth factors, and nicotine metabolites in serum. These data call for future studies detailing the cardiotoxicity of EC use in male and female youth.

Results and Discussion

Exposures and Body Weights

We hypothesized that the cardiovascular system may encounter significant detriment following EC exposure throughout the sensitive period of adolescence. We investigated this hypothesis utilizing a mouse model of “adolescent” EC exposure. According to prior studies, the adolescent period of murine development spans from post-natal day 21 to 60.²⁴ Furthermore, it has previously been shown that the murine heart continues to grow and increase its output through postnatal week 16 (4 months).²⁵ In this study, 3–5-week-old male ($n = 24-30$ per group) and female ($n = 14-22$ per group) FVB mice were exposed to EC vapor (50:50 mixture of propylene glycol and vegetable glycerin) with nicotine (20.2 mg/mL) or vehicle alone at relevant levels (one 70 mL puff per minute for 4 hrs/day, 5 days/week) for either 3 weeks or 3 months. Previously, EC users were shown to inhale 163 ± 138 puffs from their EC devices each day.²⁶ Based on these data, we intended to model heavy EC users with our exposure protocol (240 puffs per day) which falls within one standard deviation of the reported mean puffs per day. EC vapor was produced from a third-generation EC device attached to an exposure chamber (SCIREQ, Montreal, CA). Mice were exposed to HEPA-filtered air as a control (FA). Mice were exposed in batches of 3-10 mice per group over the course of approximately 2 years.

Body weights were recorded at baseline and after each month of exposure. There were no significant differences in baseline body weight across groups ($n = 15-18$ per group, not shown). For mice with body weights recorded throughout the entire exposure period ($n = 10-11$ per group, Figure 1), body weight was significantly reduced in male mice exposed to EC vapor with nicotine compared to both the EC vehicle and the FA control after 1- 2- and 3-months of exposure, with no differences across groups for female mice. Within this subset (Figure 1), male mice assigned to

the EC vehicle had baseline body weights that were significantly higher than FA; however, there were no differences among these groups by 1 month. These data indicate that EC exposure with nicotine stunts weight gain during adolescent development in a sex-dependent manner.

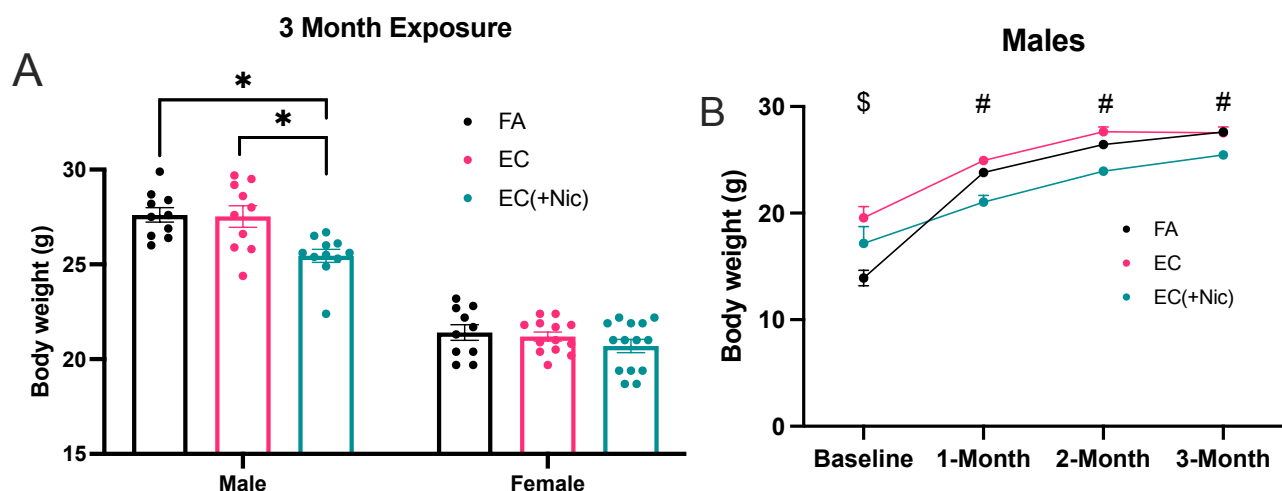


Figure 1: Body Weights: Body weights of adolescent mice exposed to either filtered air (FA), electronic cigarette vapor without nicotine (EC), or electronic cigarette vapor with nicotine (EC(+Nic)). Group sizes range from $n = 10-11$ *Panel A:* Male and female body weights following 3 months of exposure. *Panel B:* Male body weights throughout the time course of exposure. \$: EC significantly higher than FA, #: EC(+Nic) significantly reduced vs FA and EC. Data are expressed as mean \pm SEM. *, \$, #: $p < .05$ via two-way ANOVA with post-hoc Tukey's multiple comparison test

Vaping Reduces Left Ventricular Function in Young Male Mice

Male mice displayed reductions in fractional shortening and E/A ratio as measured by ultrasound (FUJIFILM Visual Sonics, Toronto, CA) after exposure to EC vapor with nicotine for 3 months, but not in response to vehicle alone (Figure 1). These changes were not found in mice exposed beginning at adulthood (3 months), female mice, mice exposed to a “casual-use” time frame (1 hr/day, 3 days/week), or mice exposed for only 3 weeks in duration (Supp. Figure 1). These results suggest that chronic e-cigarette exposure during adolescent development causes reduced systolic and diastolic cardiac function in a nicotine-dependent manner. Notably, these findings were exclusive to male adolescent mice, as adult mice unexpectedly showed a significant increase in fractional shortening, with no changes in diastolic function assessed via E/A ratio.

Right ventricular function was not affected in either sex, nor was the Fulton index, suggesting no change in RV function or RV hypertrophy (Supp. Figure 1). Systolic and diastolic blood pressure was unaffected as measured by tail-cuff (Kent Scientific)

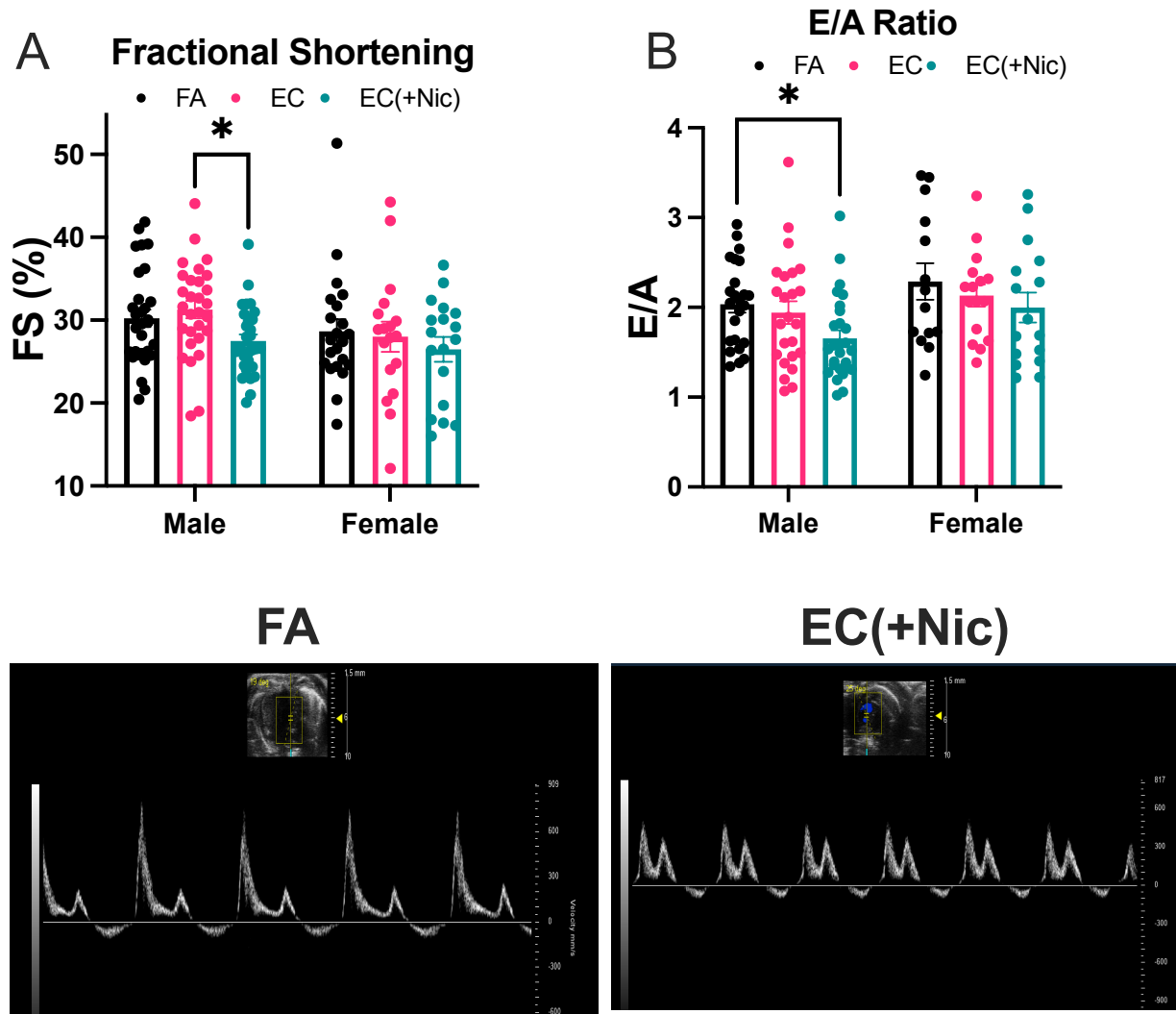


Figure 2: Left Ventricular Echocardiography. Echocardiographic analysis of the left ventricle of male and female adolescent mice after 3 months of exposure to either filtered air (FA), electronic cigarette vapor without nicotine (EC), or electronic cigarette vapor with nicotine (EC(+Nic)). Group sizes range from $n = 24-30$ for males and $n = 14-22$ for females. *Panel A:* Fractional shortening (%FS) of the left ventricle represents the percent change in left ventricular internal diameter from systole to diastole in parasternal short axis view. *Panel B:* E/A ratio of early (E) and late (A) diastolic transmitral flow velocities obtained from doppler ultrasound of mitral blood flow in apical four chamber view. Data are expressed as mean \pm SEM. *: $p < .05$ via two-way ANOVA with post-hoc Tukey's multiple comparison test. *Bottom panel:* Representative images of doppler ultrasound of mitral blood flow from FA and EC(+Nic) males. For each cardiac cycle, the heights of the first peak and second peaks were measured to obtain E and A wave velocities, respectively.

Trichrome staining of cardiac tissue in male mice revealed a distinct increase in vascular fibrosis in the vehicle group, relative to FA control and the nicotine group, implicating nicotine as a protective agent in vascular cardiac fibrosis (Figure 2). RT-qPCR performed on male LV tissue demonstrated that EC exposure with nicotine caused an increase in cardiac *COL1A1* and *COL3A1* expression after 3 weeks of exposure; however, this was reversed after 3 months of exposure (Figure 2). Whether or not alterations in collagen expression and cardiac fibrosis play a role in the observed alterations in cardiac function will require further investigation. Regardless, these results indicate that EC vapor alters extracellular matrix homeostasis in mice exposed throughout adolescent development.

To investigate whether changes in global cardiac function were associated with functional alterations at the myocyte level, cardiomyocytes were isolated after 3 months of exposure. These cardiomyocytes were stimulated *in vitro* using a Myopacer Field-Stimulator system (IonOptix, Milton, MA) and functional properties of the cells were evaluated under normal conditions and following incubation with isoproterenol. Cardiomyocyte contractility and calcium transients were not affected in male or female mice, although there was a non-significant trend ($p=.07$ via ANOVA) for reduced calcium release in male, isoproterenol challenged mice exposed to EC vapor (Supp. Figure 2). These results indicate that the observed reductions in systolic and diastolic function are more likely the result of alterations in the non-myocyte components of the heart, rather than intrinsic alterations in contractility and calcium cycling.

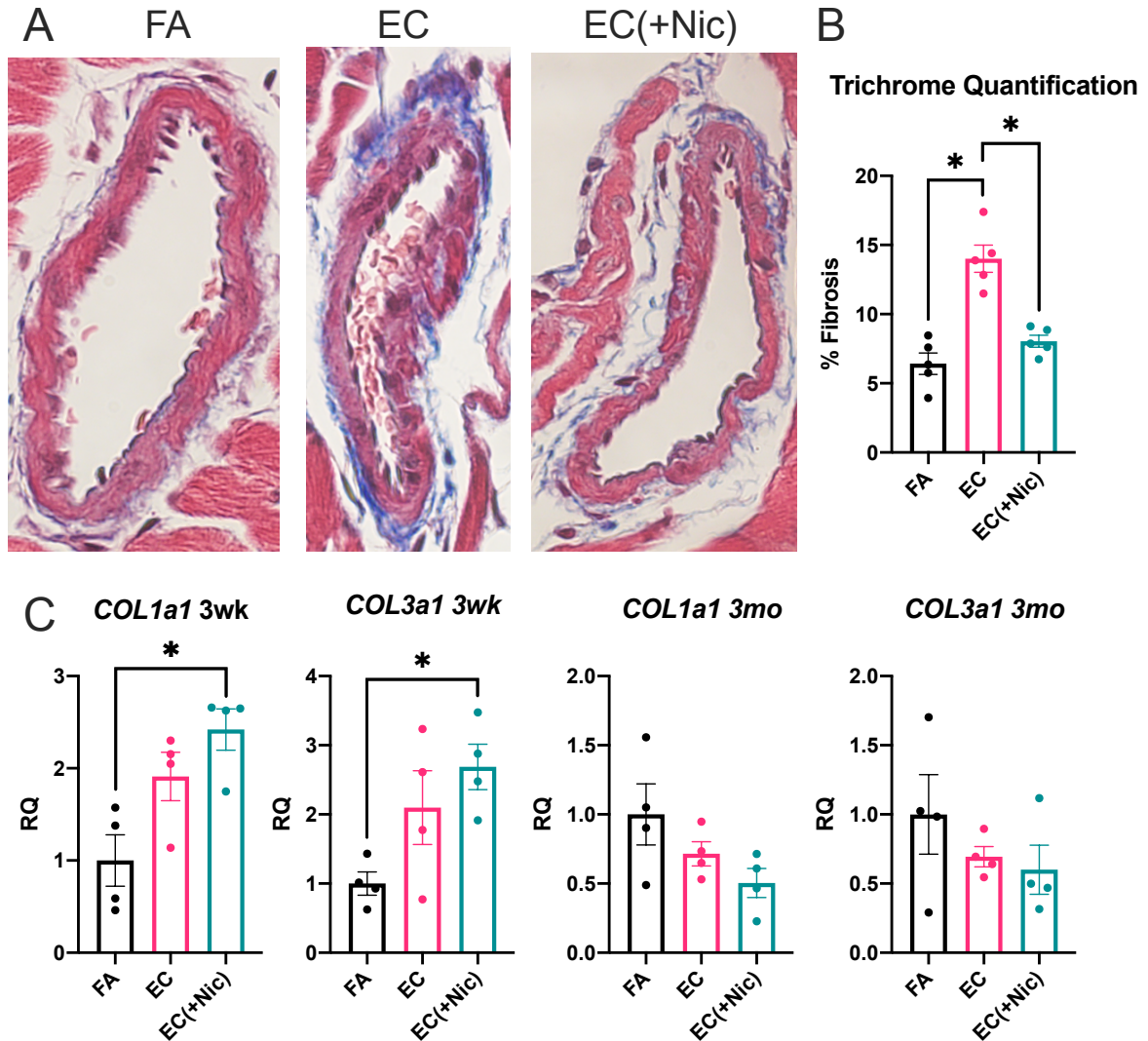


Figure 3: Assessment of Cardiac Fibrosis. *Panel A:* Representative images of cardiac blood vessels from adolescent male mice after 3 months of exposure to either filtered air (FA), electronic cigarette vapor without nicotine (EC), or electronic cigarette vapor with nicotine (EC(+Nic)). Sections were subject to Masson's trichrome stain and imaged under bright-field light microscope at 60x magnification. *Panel B:* Quantification of fibrosis from trichrome images, represented as percent area of blue staining region. Images from 5 mice per group were quantified and averaged from at least 3 images of blood vessels per mouse. *Panel C:* Relative gene expression of *COL1A1* and *COL3A1* in the left ventricle of adolescent male mice (n = 4 per group) after 3 weeks (3wk) or 3 months (3mo) of exposure measured via TaqMan-based real time quantitative polymerase chain reaction (RT-qPCR). Data are expressed as mean \pm SEM. *: $p < .05$ via one-way ANOVA with post-hoc Tukey's multiple comparison test. All statistical analysis on RT-qPCR data was performed directly on $\Delta\Delta CT$ values. $\Delta\Delta CT$ was calculated by subtracting each sample's ΔCT from the mean ΔCT from the FA control group. Relative quantity (RQ) was calculated using $RQ = 2^{-\Delta\Delta CT}$ and was normalized to the mean RQ from the FA control group.

Vaping Increases Serum Cytokines and Growth Factors

To examine the systemic changes manifested by EC, serum was analyzed for a panel of 42 cytokines by immunoassay (Ampersand Biosciences, Saranac Lake, NY). Male mice exposed to EC vapor with nicotine had significantly elevated serum interleukin (IL)-18, chemokine C-C motif chemokine ligand (CCL)2, macrophage inflammatory protein (MIP)-1 β , vascular endothelial growth factor (VEGF)-A, and stem cell factor (SCF) compared to FA (Figure 3). While several of these alterations were nicotine dependent, the EC vehicle was sufficient to cause some alterations, including MIP-1 β , SCF and VEGF-A. Females had a completely different serum cytokine profile, as only interferon (IFN) γ was increased compared to FA and EC vehicle. Thus, EC was able to drive production of markers of systemic inflammation, which may cause further downstream changes to organ systems such as the heart.

To investigate whether these systemic changes were associated with altered cardiac gene expression, RT-qPCR was performed on male mice targeting markers of inflammation and oxidative stress. Cardiac *VCAM-1* expression followed a similar pattern to *COL1A1* and *COL3A1*, showing increased expression in response to EC vapor with nicotine at 3 weeks. Following 3 months of EC exposure, *VCAM-1* expression in nicotine-exposed mice mirrored FA levels, with a significant decrease in the vehicle group (Figure 3). Although heterogeneity in the vehicle group prevented significance across groups, expression of the *TNF* and *NOS2* appeared to be increased in response to EC exposure with nicotine at 3 weeks (Figure 4). By 3 months, *TNF* expression was significantly decreased in nicotine-exposed mice, and *NOS2* expression returned to near-FA levels. *VCAM-1* encodes vascular cell adhesion protein 1, a cytokine-inducible adhesion molecule that allows leukocytes to migrate from blood vessels into resident tissues.²⁷ *TNF* and *NOS2* encode the proinflammatory cytokine, tumor necrosis factor alpha, and the pro-oxidative stress enzyme,

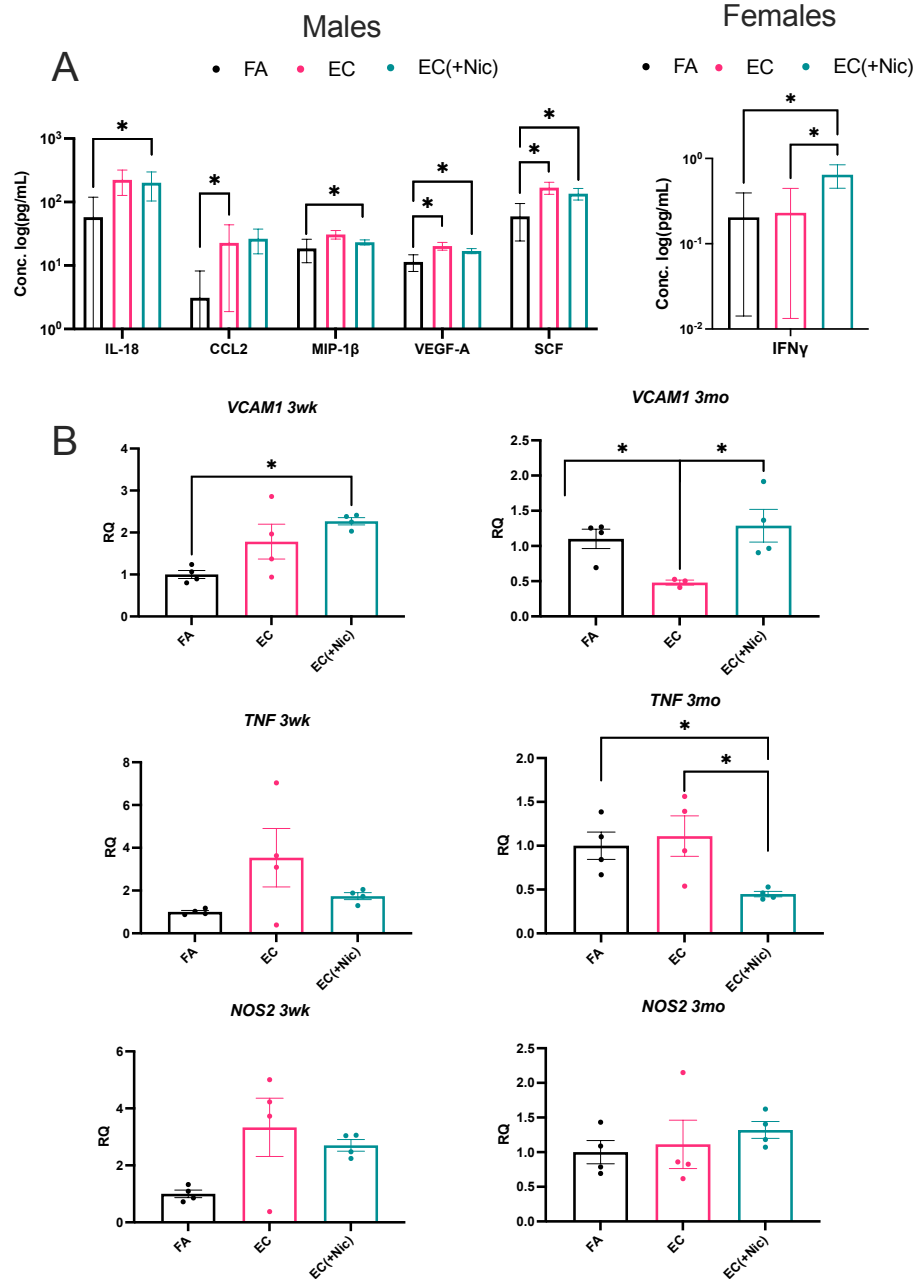


Figure 4: Assessment of Systemic and Cardiac Biomarkers. *Panel A:* Concentration of various cytokines in the serum collected from male and female mice via cardiac puncture within 24 hours of exposure to either filtered air (FA) (n=6 male, 5 female), e-cigarette vapor without nicotine (EC) (n=3 male, 4 female), or e-cigarette vapor with nicotine (EC(+Nic)) (n=5 male and female), A panel of 42 cytokines/growth factors were quantified. Biomarkers with significant alterations include interleukin 18 (IL-18), C-C motif chemokine ligand 2 (CCL2), macrophage inflammatory protein 1 β (MIP-1 β), vascular endothelial growth factor A (VEGF-A), stem cell factor (SCF), and interferon gamma (IFN γ). *Panel B:* Relative gene expression of *VCAM1*, *TNF*, and *NOS2* in the left ventricle of adolescent male mice (n = 4 per group) after 3 weeks (3wk) or 3 months (3mo) of exposure measured via TaqMan-based real time quantitative polymerase chain reaction (RT-qPCR). Data are expressed as mean \pm SEM. *: p<.05 via one-way ANOVA with post-hoc Tukey's multiple comparison test. All statistical analysis on RT-qPCR data was performed directly on Δ CT values.

inducible nitric oxide synthase 2, respectively. Taken together, these data suggest that EC vapor exposure with nicotine may promote both a systemic and cardiac pro-inflammatory state in male mice exposed throughout adolescent development.

Female Mice Display Faster Rates of Nicotine Metabolism Than Males

Given the many nicotine- and sex-dependent results noted in this study, we next sought to determine whether nicotine metabolism was different between males and females. While nicotine concentrations in serum of male and female mice exposed to EC with nicotine were similar, concentrations of metabolites including cotinine and 3-hydroxycotinine (3HC) were significantly lower in female mice compared to males (Figure 4). Further, the 3HC/cotinine ratio, a measure of cytochrome P450 2A6 (Cyp2A5 in mice) activity²⁸, a critical enzyme in nicotine metabolism, was significantly and substantially increased in female mice (Figure 4). RT-qPCR of liver tissue targeting Cyp2A5 also showed increased expression in females as compared to males (Figure 4), further supporting a more rapid nicotine metabolism in female mice. Due to the fact that reductions in cardiac function and body weight were only observed in male mice exposed to EC vapor with nicotine, this finding could suggest that females exhibit some degree of protection against EC vapor as a result of enhanced nicotine metabolism.

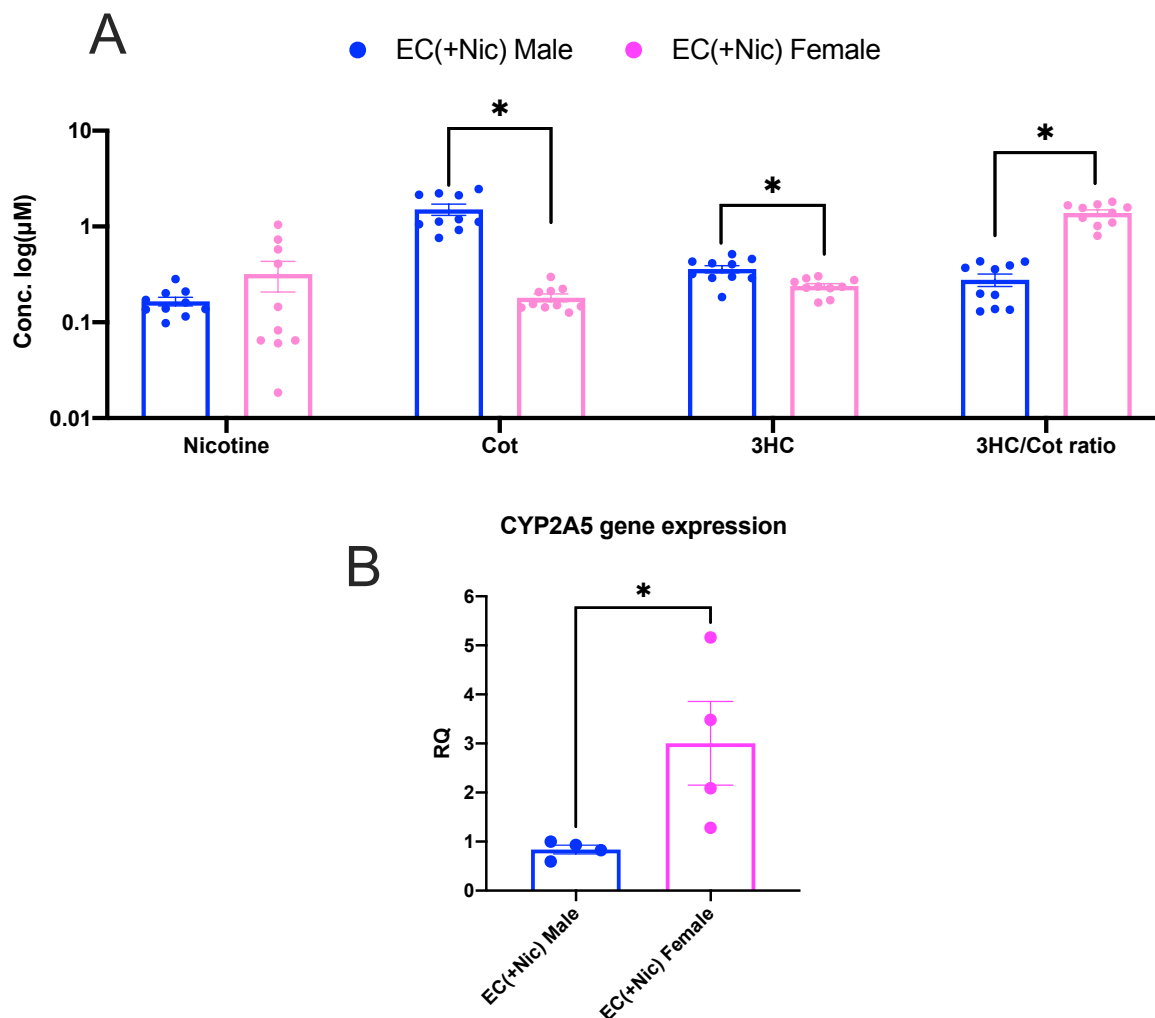


Figure 5: Nicotine Metabolism. *Panel A:* Concentration of nicotine and its metabolites in serum of male and female mice exposed for 3 months to electronic cigarette vapor with nicotine (EC(+Nic)) (n=10 per group) collected via submandibular bleed within 4 hours of exposure. Measurements were obtained via liquid chromatography-mass spectrometry (LC-MS). Measurements include nicotine, cotinine (cot), and 3-hydroxycotinine (3HC). *Panel B:* Relative gene expression of *CYP2A5* in the liver of adolescent male and female mice (n = 4 per group) after 3 months of exposure measured via TaqMan-based real time quantitative polymerase chain reaction (RT-qPCR). Data are expressed as mean \pm SEM. *: $p < .05$ via unpaired, two-tailed student's t-test. All statistical analysis on RT-qPCR data was performed directly on Δ CT values.

Conclusions

To our knowledge, this is the first study to evaluate cardiac function coupled with biomarkers of harm in young mice exposed to EC vapor. Our results heighten the concern for the dangers of EC use, specifically in youth, and call for further work detailing the mechanistic

contributions to the observed reduction in cardiac function. While EC vapor alone was not shown to induce functional cardiac alterations, a synergistic effect of nicotine and its metabolites with reactive by-products of combustion, such as various aldehydes, could account for the observed effects. Regardless, the novel results of this study demonstrate that EC vapor exposure with nicotine can reduce cardiac function in developing male mice.

Materials and Methods

Animals, Exposures, and Tissue Collection

All animals were handled according to NIH guidelines under Institutional Animal Care and Use Committee (IACUC) protocols approved at The Ohio State University, Columbus, Ohio. FVB male and female mice were housed for at least 1 week in our facility before breeding. FVB offspring were aged to 3-5 weeks old in our facility before the start of exposure. Following 2 days (1hr/day) of acclimation to the exposure chambers, adolescent mice (3-5 weeks old on day 1 of exposure) were exposed to EC vapor (50:50 mixture of propylene glycol and vegetable glycerin) with nicotine (20.2 mg/mL) or vehicle alone (one 70 mL puff per minute for 4 hrs/day, 5 days/week) for either 3 weeks or 3 months. EC vapor was produced from a third-generation EC device attached to an exposure chamber (SCIREQ, Montreal, CA). Mice were exposed to HEPA-filtered air as a control (FA). Blood pressure was recorded via tail-cuff (Kent Scientific). Body weight was recorded for each mouse within 1 week prior to the exposure start date and was recorded again after each month of exposure. Serum used for nicotine metabolism analysis was obtained via submandibular bleed within 4 hours of exposure. Serum used for cytokine immunoassay was obtained via cardiac puncture within 24 hours of exposure. Mice were euthanized, and heart tissue was either fixed in 4% paraformaldehyde, or divided into individual chambers and snap frozen using liquid nitrogen. The Fulton index was calculated as the weight

ratio: $(RV/(LV+Septum))$). Liver tissue was also collected and snap frozen in liquid nitrogen. Fixed tissue was transferred to 70% ethyl alcohol, paraffin embedded, and cut into 5- μ m sections. Paraffin-embedded hearts were cut from the base to the apex.

Echocardiography

Echocardiographic assessments were performed using a 40-MHz transducer (Vevo 3100; Visualsonics, Toronto, Ontario, Canada). Mice were anesthetized with 1% isoflurane in 100% O₂ through a nose cone, and internal body temperature was maintained at 37°C throughout the assessment. Following induction of anesthesia and after the heart rate of the animal returned to normal (400–550 beats per minute [bpm]), parasternal short-axis views were obtained using a 15-MHz probe. Cine loops collected from M mode views were analyzed for left ventricular (LV) systolic and diastolic internal dimensions (LVESd and LVEDd) and diameter of the pulmonary valve (PV_d). Percent fractional shortening (%FS) was calculated using the equation: $\%FS = [(LVEDd - LVESd) / LVEDd \times 100]$. Additionally, cine loops of blood flow velocity through the pulmonary valve and mitral valve were obtained via pulse wave doppler measurements from the parasternal short-axis view and apical four chamber view, respectively. Cine loops of pulmonary blood flow velocity were analyzed for a trace of the velocity time integral (VTI). Right ventricular (RV) stroke volume (SV) was estimated using the equation $SV = [0.785 \times PV_d \times VTI]$ and RV cardiac output (CO) was obtained by multiplying SV by heart rate. Cine loops of blood flow through the mitral valve were analyzed for early (E) and late (A) diastolic transmitral flow velocities. Transmitral E/A ratio was calculated as a ratio of the two measurements. When obtaining cine loops of blood flow velocity through the mitral valve, occasionally heart rate needed to be lowered below 400 bpm to achieve separation of the E and A waves. Data were averaged from at least 3 cardiac cycles per mouse for all measurements and calculations.

Masson's Trichrome Staining

Heart sections were stained with hematoxylin, Beibrich's scarlet acid, and Aniline blue solution from Trichrome Staining Kit Assay (Abcam, Cambridge, United Kingdom) following instructions from the supplier. A minimum of 3 perivascular images per mouse were captured using bright-field light microscopy with 60X magnification. Percent fibrosis was calculated using ImageJ software (National Institutes of Health, Washington DC). Color images were separated via color deconvolution for the identification of collagen fibers. Collagen fibers were then highlighted by adjusting the threshold tool, and percent area was calculated using the measurement tool. Data from 3-5 images per mouse were averaged to obtain a single percent area value for each mouse.

Cardiomyocyte Isolation and Measurement of Sarcomere Function and Intracellular Ca^{2+} Transients.

Cardiomyocytes were isolated as previously described.²⁹ Briefly, hearts were removed and retrogradely perfused through the aorta with Liberase and trypsin until digested. Isolated cells were then plated on laminin-coated glass-bottom inserts (Cell MicroControls, Norfolk, VA) for functional analyses. Glass-bottom inserts were perfused with warm contractile buffer within a flow chamber attached to an Olympus IX-71 microscope. Cells were stimulated (1 Hz, 3-ms duration) with a Myopacer Field-Stimulator system (IonOptix, Milton, MA), and functional properties of the cells were evaluated using the Sarclen Sarcomere Length Acquisition Module with a Myocam-S Digital CCD camera video imaging system (IonOptix). Analyses of 10-15 cells from each mouse provided the parameters of sarcomere percent peak shortening (normalized to baseline length, %PS; cellular equivalent of %FS), sarcomere maximal departure, return velocities ($\pm dl/dt$), and sarcomere time-to-90% PS and relengthening (TPS₉₀ and TR₉₀, respectively). For Ca^{2+} measurements, cardiomyocytes in glass-bottom dishes were loaded with fura-2 AM (0.5 μM)

for 20 min at 25°C and then washed and treated with normal culture media for 20 min at 25°C. Fluorescence was recorded in stimulated cardiomyocytes using a dual-excitation, single-emission system (IonOptix). Transients were analyzed for values of calcium release (TPS₉₀) and reuptake (τ , TR₉₀). To measure the effect of β -adrenergic stimulation on contractility and Ca²⁺ transients, cells were treated with in 10⁻⁷ M isoproterenol for 10 min prior to assessment.

Quantitative Real-Time PCR

Total RNA was isolated from snap frozen left ventricular heart tissue or liver tissue from 3-week and 3-month exposed mice using the TRIzol Reagent (Invitrogen, Carlsbad, CA) following instructions from the supplier, and concentrations were determined using a NanoDrop 2000c (ThermoScientific, Wilmington, DE). 500 ng of RNA was reverse transcribed to generate cDNA using SuperScript IV VILO Master Mix with ezDNase Enzyme (Invitrogen, Carlsbad, CA) using the QuantStudio 3 Real-Time PCR System (Applied Biosystems, Foster City, CA) as a thermocycler. Real-time PCR was performed using the QuantStudio 3 Real-Time PCR System, TaqMan Fast Advanced Master Mix (Applied Biosystems, Foster City, CA), and TaqMan gene expression assays for mouse: *COL1A1* (assay ID: Mm00801666_g1), *COL3A1* (assay ID: Mm00802300_m1), *VCAM-1* (assay ID: Mm01320969_g1), *TNF* (assay ID: Mm00443258_m1), *NOS2* (assay ID: Mm00440502_m1), and *CYP2A5* (Mm00487248_g1). Either *18S* (assay ID: Mm04277571_s1) or *GAPDH* (assay ID: Mm99999915_g1) were used as endogenous controls. PCR reactions contained 4 ng cDNA (total RNA equivalent) of each sample in triplicate.

All statistical analyses were conducted on Δ CT values. $\Delta\Delta$ CT was calculated by subtracting each sample's Δ CT from the mean Δ CT from the FA control group. Relative quantity (RQ) was calculated using $RQ = 2^{-\Delta\Delta CT}$ and was normalized to the mean RQ from the FA control group.

Cytokine Immunoassay Panel

Serum samples were shipped on dry ice to undergo analysis via Mouse MAP 4.1- Sample Testing (Ampersand Biosciences, Saranac Lake, NY). All concentrations below the limit of detection were set to a concentration of 0. One male biological replicate from the vehicle group was excluded from all analyses due to consistently low or undetectable levels across several unrelated markers (e.g. insulin, interleukin-5, and VEGF-A).

Nicotine Metabolism Assessments Using Liquid Chromatography-Mass Spectrometry

Nicotine, nicotine-methyl-d₃(Nic-d₃), cotinine, and cotinine-methyl-d₃(Cot-d₃) were purchased from Sigma-Aldrich (St Louis, MO). trans-3'-Hydroxycotinine (3HC), trans-3-Hydroxycotinine-methyl-d₃ (3HC-d₃), nicotine-N-glucuronide (Nic-Gluc), nicotine-methyl-d₃-N-glucuronide (Nic-Gluc-d₃), cotinine-N-glucuronide (Cot-Gluc), cotinine-methyl-d₃-N-glucuronide (Cot-Gluc-d₃), trans-3'-hydroxycotinine O-β-D-glucuronide (3HC-Gluc), rac trans-3'-hydroxycotinine-d₃ O-β-D-glucuronide (3HC-Gluc-d₃), nicotine-N'-oxide (Nic-O), nicotine-N'-oxide-d₃ (Nic-O-D₃), cotinine-N-oxide (Cot-O), cotinine-N-oxide-d₃ (Cot-O-d₃), rac 4-hydroxy-4-(3-pyridyl) butanoic acid (4HPBA) dicyclohexylamine salt, and rac 4-hydroxy-4-(3-pyridyl) butanoic-d₃ acid (4HPBA-d₃) dicyclohexylamine salt were purchased from Toronto Research Chemicals (Toronto, ON, Canada). Liquid chromatography-mass spectrometry (LC-MS) grade acetonitrile, ammonium formate and formic acid were purchased from Fisher Scientific (Fair Lawn, NJ). Ultrapure Millipore water was from the Milli-Q Ultrapure water system.

For analysis of serum specimens, 5 µl aliquots of each specimen were spiked with 5 µl of an internal standard mixture that included 0.1 µg/mL of Nic-d₃, Cot-d₃, 3HC-d₃, Nic-Gluc-d₃, Cot-Gluc-d₃, 3HC-O-Gluc-d₃, Nic-O-d₃, Cot-O-d₃, and 4HPBA-d₃. After the addition of 30 µl of acetonitrile, the mixture was vortexed thoroughly. All precipitate was removed by centrifugation

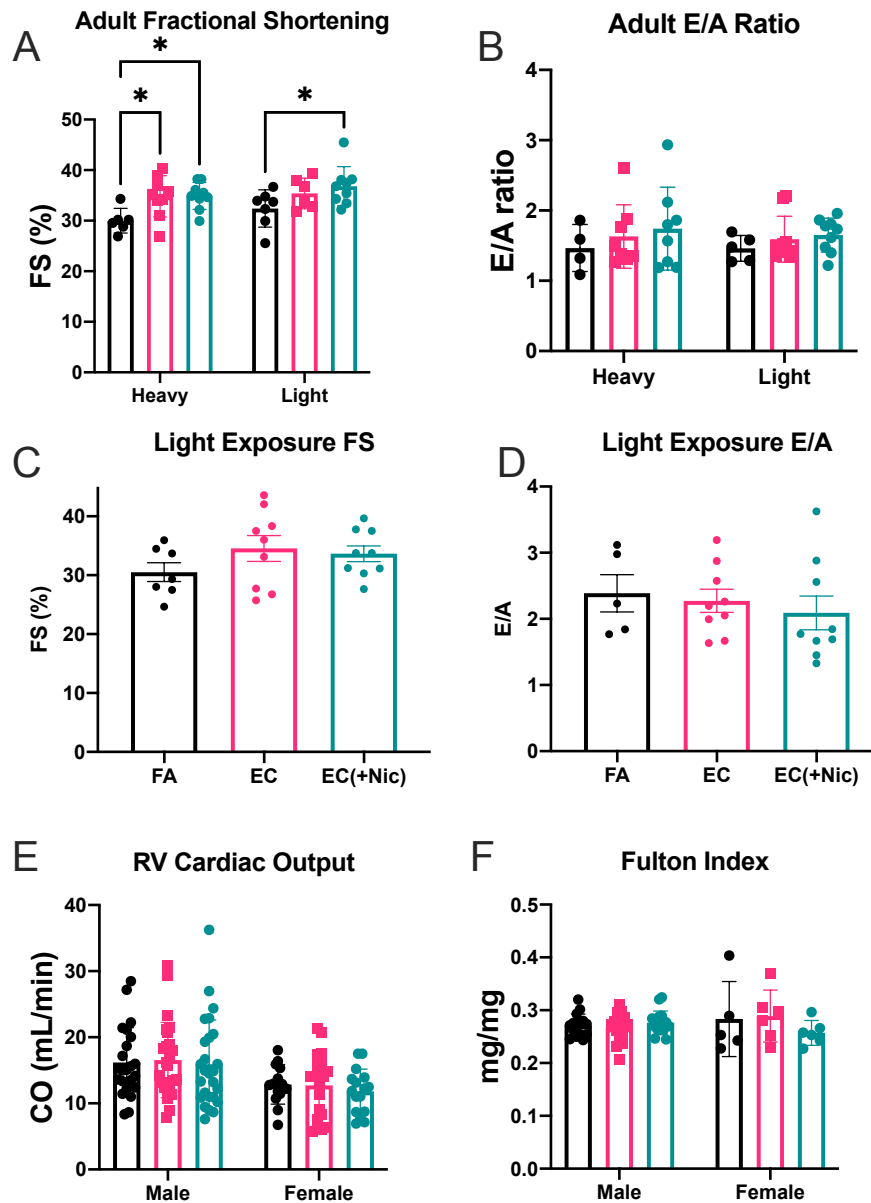
at 16,000 g for 10 min at 4°C. The supernatant was transferred into 350 µl conical glass sample vials for LC-MS analysis. Serum nicotine and its metabolites were detected and quantified using the Acquity ultra performance liquid chromatography (UPLC) system (Waters Corporation, Milford, MA) with a high strength silica T3 (100 X 2.1 mm, 1.8 µm) UPLC column and a Xevo G2-S Qtof mass spectrophotometer. The LC method was performed using a 2 µl sample injection volume, a 50°C column temperature and a flow rate of 0.4mL/min under the following conditions: a 4 min linear gradient of 98% buffer A (5 mM ammonium formate with 0.01% formic acid) to 90% buffer A: 10% buffer B (100% acetonitrile), a subsequent gradient to 95% buffer B in 0.5 min, followed by 1minute at 95% B. The column was re-equilibrated for one minute at initial conditions before the next sample injection.

The Waters Xevo G2-S Qtof MS was operated in positive electrospray ionization MS sensitive mode, with capillary voltage at 0.6 kV. Nitrogen was used for both cone and desolvation gases at 50 L/h and 800 L/h, respectively. The source temperature was 130°C, desolvation gas temperature was 500°C. The dwell time was 0.1 sec. The cone voltage was 15 V. The mass range was 100-1000. The m/z traces for quantification of each compound and respective d3-labeled internal standards (IS) and peak retention time are: 163.12 (IS: 166.14), 2.17 minutes for nicotine; 177.10 (IS: 180.12), 4.02 min for cotinine; 193.10 (IS: 196.12), 2.76 min for 3HC; 339.15 (IS: 342.17), 0.63 min for Nic-Gluc; 353.14 (IS: 356.16), 0.75 min for Cot-Gluc; 369.13 (IS: 372.15), 1.73 min for 3HC-Gluc; 179.12 (IS: 182.14), 2.61 min for Nic-O; 193.10 (IS: 196.12), 2.25 min for Cot-O; and 182.08 (IS: 185.10) 1.71 min for 4HPBA, respectively. The low quantification limit for each compound was similar, each at approximately 0.02 µM.

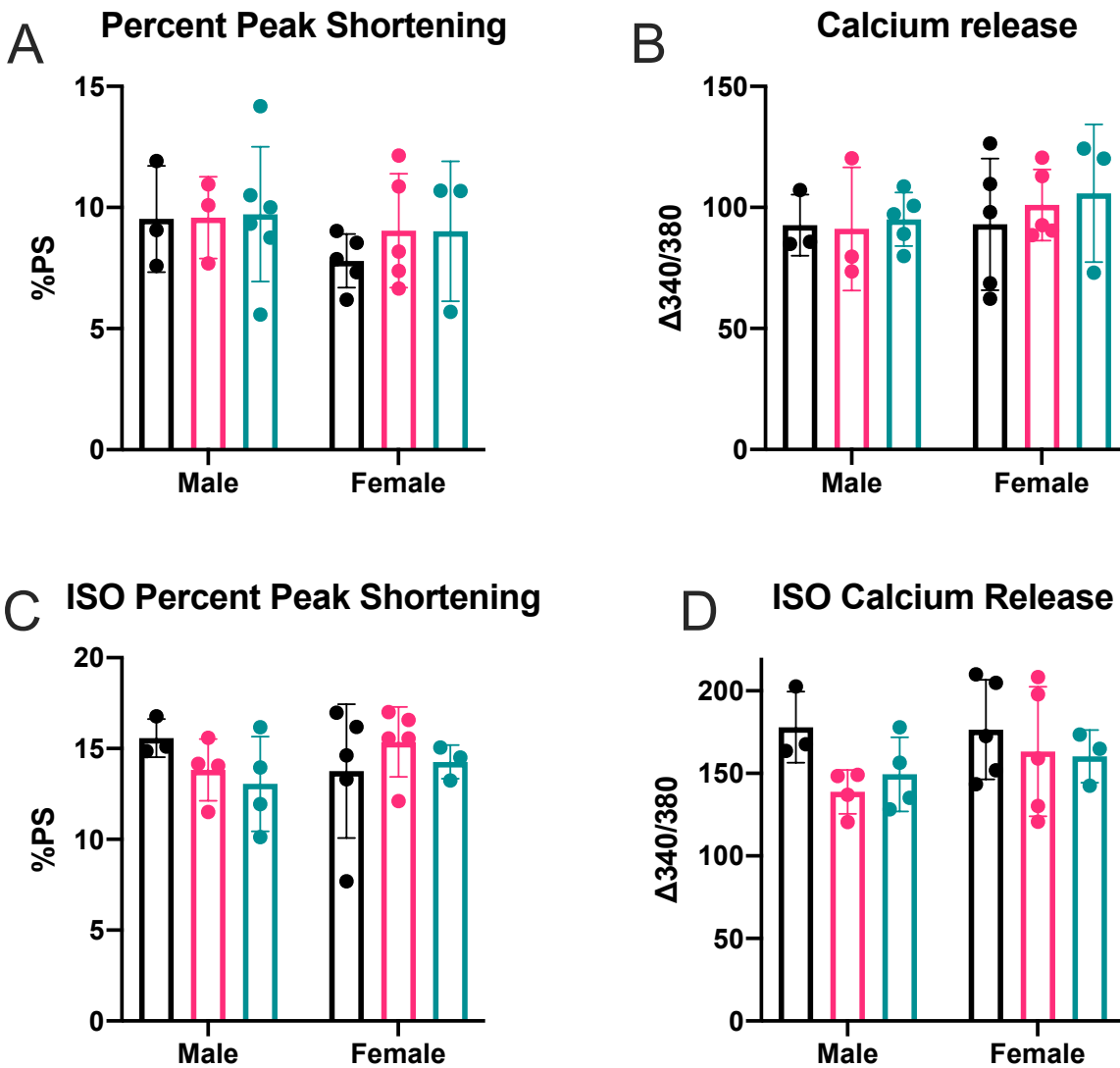
Statistical Analysis

All data are reported as mean \pm SEM. Data were graphed and analyzed using GraphPad Prism (Version 9; GraphPad Software Inc, San Diego, CA). Statistical analysis among groups was assessed using either an unpaired, two-tailed Student's t-test or a one- or two-way ANOVA with post-hoc analysis vis Tukey's multiple comparison test. The values were considered statistically significant with $P < 0.05$.

Supplemental Figures



Supplemental Figure 1: Additional Measures of Global Cardiac Function. *Panel A:* Fractional Shortening (%FS) of adult mice (3 months old) exposed for 3 months to either filtered air (FA, black), electronic cigarette vapor without nicotine (EC, pink) or electronic cigarette vapor with nicotine (EC(+Nic), green) for either 4 hours per day (light) or 4 hours per day (heavy). *Panel B:* E/A ratio of early (E) and late (A) diastolic transmitral flow velocities. *Panels C and D:* %FS and E/A ratio in adolescent mice (1 month old) exposed for 3 months for 1 hour per day (Light exposure). *Panel E:* Cardiac output (CO) from the right ventricle of adolescent mice exposed for 4 hours per day for 3 months. *Panel F:* Fulton index (index of RV hypertrophy) of male and female adolescent mice exposed for 4 hours per day for 3 months. Data are expressed as mean \pm SEM. *: $p < .05$ via one- or two-way ANOVA with post-hoc Tukey's multiple comparison test.



Supplemental Figure 2: Cardiomyocyte Function. Functional data from cardiomyocytes isolated from male and female adolescent mice exposed to either filtered air (FA, black), e-cigarette vapor without nicotine (EC, pink), or e-cigarette vapor with nicotine (EC(+Nic), green) for 3 months. *Panel A:* Percent peak shortening (%PS) of cardiomyocyte sarcomeres. *Panel B:* Magnitude of calcium release measured as a change in fluorescence ratio between 340nm and 380nm. *Panels C and D:* %PS and magnitude of calcium release in cardiomyocytes treated with isoproterenol.

References

1. Singh T, Arrazola RA, Corey CG, et al. Tobacco Use Among Middle and High School Students — United States, 2011–2015. *MMWR Morb Mortal Wkly Rep.* 2016;65(14):361-367. doi:10.15585/mmwr.mm6514a1
2. Miech R, Johnston L, O'Malley PM, Bachman JG, Patrick ME. Trends in Adolescent Vaping, 2017–2019. *N Engl J Med.* 2019;381(15):1490-1491. doi:10.1056/nejmc1910739
3. McConnell R, Barrington-Trimis JL, Wang K, et al. Electronic cigarette use and respiratory symptoms in adolescents. *Am J Respir Crit Care Med.* 2017;195(8):1043-1049. doi:10.1164/rccm.201604-0804OC
4. Tsai MC, Song MA, McAndrew C, et al. Electronic versus combustible cigarette effects on inflammasome component release into human lung. *Am J Respir Crit Care Med.* 2019;199(7):922-925. doi:10.1164/rccm.201808-1467LE
5. Chaumont M, van de Borne P, Bernard A, et al. Fourth generation e-cigarette vaping induces transient lung inflammation and gas exchange disturbances: Results from two randomized clinical trials. *Am J Physiol - Lung Cell Mol Physiol.* 2019;316(5):L705-L719. doi:10.1152/ajplung.00492.2018
6. Meo SA, Ansary MA, Barayan FR, et al. Electronic Cigarettes: Impact on Lung Function and Fractional Exhaled Nitric Oxide Among Healthy Adults. *Am J Mens Health.* 2019;13(1). doi:10.1177/1557988318806073
7. Anderson C, Majeste A, Hanus J, Wang S. E-cigarette aerosol exposure induces reactive oxygen species, DNA damage, and cell death in vascular endothelial cells. *Toxicol Sci.* 2016;154(2):332-340. doi:10.1093/TOXSCI/KFW166
8. Hom S, Chen L, Wang T, Ghebrehwet B, Yin W, Rubenstein DA. Platelet activation,

- adhesion, inflammation, and aggregation potential are altered in the presence of electronic cigarette extracts of variable nicotine concentrations. *Platelets*. 2016;27(7):694-702. doi:10.3109/09537104.2016.1158403
9. Qasim H, Karim ZA, Silva-Espinoza JC, et al. Short-term E-cigarette exposure increases the risk of thrombogenesis and enhances platelet function in mice. *J Am Heart Assoc*. 2018;7(15). doi:10.1161/JAHA.118.009264
 10. Olfert IM, De Vallance E, Hoskinson H, et al. Chronic exposure to electronic cigarettes results in impaired cardiovascular function in mice. *J Appl Physiol*. 2018;124(3):573-582. doi:10.1152/jappphysiol.00713.2017
 11. Schweitzer KS, Chen SX, Law S, et al. Endothelial disruptive proinflammatory effects of nicotine and e-cigarette vapor exposures. *Am J Physiol - Lung Cell Mol Physiol*. 2015;309(2):L175-L187. doi:10.1152/ajplung.00411.2014
 12. Shi H, Fan X, Horton A, et al. The Effect of Electronic-Cigarette Vaping on Cardiac Function and Angiogenesis in Mice. *Sci Rep*. 2019;9(1):1-9. doi:10.1038/s41598-019-40847-5
 13. Olfert IM, De Vallance E, Hoskinson H, et al. Chronic exposure to electronic cigarettes results in impaired cardiovascular function in mice. *J Appl Physiol*. 2018;124(3):573-582. doi:10.1152/jappphysiol.00713.2017
 14. De Oliveira-Fonoff AM, Mady C, Pessoa FG, et al. The role of air pollution in myocardial remodeling. *PLoS One*. 2017;12(4):e0176084. doi:10.1371/journal.pone.0176084
 15. Crotty Alexander LE, Drummond CA, Hepokoski M, et al. Chronic inhalation of e-cigarette vapor containing nicotine disrupts airway barrier function and induces systemic inflammation and multiorgan fibrosis in mice. *Am J Physiol - Regul Integr Comp Physiol*.

- 2018;314(6):R834-R847. doi:10.1152/ajpregu.00270.2017
16. Boor P, Casper S, Celec P, et al. Renal, vascular and cardiac fibrosis in rats exposed to passive smoking and industrial dust fibre amosite. *J Cell Mol Med*. 2009;13(11-12):4484-4491. doi:10.1111/j.1582-4934.2008.00518.x
 17. *Public Health Consequences of E-Cigarettes*. National Academies Press; 2018. doi:10.17226/24952
 18. Son Y, Mishin V, Laskin JD, et al. Hydroxyl Radicals in E-Cigarette Vapor and E-Vapor Oxidative Potentials under Different Vaping Patterns. *Chem Res Toxicol*. 2019;32(6):1087-1095. doi:10.1021/acs.chemrestox.8b00400
 19. Nelin TD, Joseph AM, Gorr MW, Wold LE. Direct and indirect effects of particulate matter on the cardiovascular system. *Toxicol Lett*. 2012;208(3):293-299. doi:10.1016/j.toxlet.2011.11.008
 20. Nemmar A, Hoet PHM, Vanquickenborne B, et al. Passage of inhaled particles into the blood circulation in humans. *Circulation*. 2002;105(4):411-414. doi:10.1161/hc0402.104118
 21. Buchanan ND, Grimmer JA, Tanwar V, Schwieterman N, Mohler PJ, Wold LE. Cardiovascular risk of electronic cigarettes: A review of preclinical and clinical studies. *Cardiovasc Res*. 2020;116(1):40-50. doi:10.1093/cvr/cvz256
 22. Gorr MW, Velten M, Nelin TD, Wold LE, Sun Q, Wold LE. Early life exposure to air pollution induces adult cardiac dysfunction. *Am J Physiol - Hear Circ Physiol*. 2014;307(9):H1353-H1360. doi:10.1152/ajpheart.00526.2014
 23. Tanwar V, Gorr MW, Velten M, et al. In Utero Particulate Matter Exposure Produces Heart Failure, Electrical Remodeling, and Epigenetic Changes at Adulthood. *J Am Heart*

- Assoc.* 2017;6(4). doi:10.1161/JAHA.117.005796
24. Laviola G, Macrì S, Morley-Fletcher S, Adriani W. Risk-taking behavior in adolescent mice: Psychobiological determinants and early epigenetic influence. In: *Neuroscience and Biobehavioral Reviews*. Vol 27. Elsevier Ltd; 2003:19-31. doi:10.1016/S0149-7634(03)00006-X
 25. Wiesmann F, Ruff J, Hiller K-H, Rommel E, Haase A, Neubauer S. Developmental changes of cardiac function and mass assessed with MRI in neonatal, juvenile, and adult mice. *Am J Physiol Circ Physiol*. 2000;278(2):H652-H657. doi:10.1152/ajpheart.2000.278.2.H652
 26. Dautzenberg B. Real-Time Characterization of E-Cigarettes Use: The 1 Million Puffs Study. *J Addict Res Ther*. 2015;06(02):1-5. doi:10.4172/2155-6105.1000229
 27. Wennerås C, Matsumoto K, Bochner BS, et al. Eosinophil Trafficking. In: *Eosinophils in Health and Disease*. Elsevier Inc.; 2013:121-166. doi:10.1016/B978-0-12-394385-9.00006-7
 28. Tanner JA, Novalen M, Jatlow P, et al. Nicotine metabolite ratio (3-Hydroxycotinine/Cotinine) in plasma and urine by different analytical methods and laboratories: Implications for clinical implementation. *Cancer Epidemiol Biomarkers Prev*. 2015;24(8):1239-1246. doi:10.1158/1055-9965.EPI-14-1381
 29. Norby FL, Wold LE, Duan J, Hintz KK, Ren J. IGF-I attenuates diabetes-induced cardiac contractile dysfunction in ventricular myocytes. *Am J Physiol Metab*. 2002;283(4):E658-E666. doi:10.1152/ajpendo.00003.2002